REGULAR ARTICLE

blood advances

Inducible *Sbds* deletion impairs bone marrow niche capacity to engraft donor bone marrow after transplantation

Ji Zha,[1] Lori K. Kunselman,[1] Hongbo M. Xie,[2] Brian Ennis,[2] Yash B. Shah,[1] Xia Qin,[1,3] Jian-Meng Fan,[4] Daria V. Babushok,[4,5] and Timothy S. Olson[1,4,5]

[1]Cell Therapy and Transplant Section, Division of Oncology, Department of Pediatrics, and [2]Department of Biomedical Health Informatics, Children's Hospital of Philadelphia, Philadelphia, PA; [3]Department of Hematology and Oncology, National Children's Medical Center, Shanghai Children's Medical Center, Shanghai, China; [4]Comprehensive Bone Marrow Failure Center, Children's Hospital of Philadelphia, Philadelphia, PA; and [5]Perelman School of Medicine, University of Pennsylvania, Philadelphia, PA

Key Points

- Induction of *Sbds* deficiency in recipient BM niche cells impairs efficient engraftment of healthy donor HSC after transplantation.
- SBDS deficiency impairs multiple cellular signaling pathways in post-myeloablation marrow niches critical for restoration of hematopoiesis.

Bone marrow (BM) niche-derived signals are critical for facilitating engraftment after hematopoietic stem cell (HSC) transplantation (HSCT). HSCT is required for restoration of hematopoiesis in patients with inherited BM failure syndromes (iBMFSs). Shwachman-Diamond syndrome (SDS) is a rare iBMFS associated with mutations in *SBDS*. Previous studies have demonstrated that SBDS deficiency in osteolineage niche cells causes BM dysfunction that promotes leukemia development. However, it is unknown whether BM niche defects caused by SBDS deficiency also impair efficient engraftment of healthy donor HSC after HSCT, a hypothesis that could explain morbidity noted after clinical HSCT for patients with SDS. Here, we report a mouse model with inducible *Sbds* deletion in hematopoietic and osteolineage cells. Primary and secondary BM transplantation (BMT) studies demonstrated that SBDS deficiency within BM niches caused poor donor hematopoietic recovery and specifically poor HSC engraftment after myeloablative BMT. We have also identified multiple molecular and cellular defects within niche populations that are driven by SBDS deficiency and are accentuated by or develop specifically after myeloablative conditioning. These abnormalities include altered frequencies of multiple niche cell subsets, including mesenchymal lineage cells, macrophages, and endothelial cells; disruption of growth factor signaling, chemokine pathway activation, and adhesion molecule expression; and p53 pathway activation and signals involved in cell cycle arrest. Taken together, this study demonstrates that SBDS deficiency profoundly impacts recipient hematopoietic niche function in the setting of HSCT, suggesting that novel therapeutic strategies targeting host niches could improve clinical HSCT outcomes for patients with SDS.

Introduction

Maintenance of hematopoietic stem cells (HSC) and downstream regulation of hematopoiesis rely upon tightly orchestrated signals generated from specialized bone marrow (BM) microenvironments known as niches. Studies over the past 2 decades have identified multiple BM niche cells that regulate HSC homeostasis, including mesenchymal stem cells (MSCs), osteolineage cells (OCs), endothelial cells (ECs), adipocytes, macrophages, megakaryocytes, and Schwann cells.[1,2] These niche-derived signals not only are important for homeostatic hematopoiesis but also play critical roles in facilitating engraftment

Submitted 2 March 2021; accepted 17 August 2021; prepublished online on *Blood Advances* First Edition 8 October 2021; final version published online 4 January 2022. DOI 10.1182/bloodadvances.2021004640.

The data in this project, including raw sequencing data, are registered to BioProject (accession number PRJNA763892).

For other original data, please contact olsont@chop.edu.

The full-text version of this article contains a data supplement.

after HSC transplantation (HSCT). Murine models in which selected niche components are disrupted demonstrate impaired donor HSC engraftment after HSCT.[3,4]

Inherited BM failure syndromes (iBMFS) are caused by germline genetic mutations in genes long known to have cell autonomous impacts on HSC and progenitor (HSPC) function. Patients with iBMFS require HSCT for cure of BM failure (BMF) or hematopoietic lineage deficiency, or for prevention/treatment of myelodysplastic syndrome (MDS). Recently, studies using animal models of human iBMFSs have demonstrated that hematopoietic dysfunction may arise as a result of nonautonomous mechanisms resulting from impacts of the underlying germline mutation within BM niche cell populations.[5-9] Our group has previously demonstrated that BM niche capacity to engraft healthy donor HSC after transplantation is impaired in some iBMFSs because of mutation effects within niche cells or preexistence of BMF.[4,10]

SDS is a rare iBMFS caused in most cases by biallelic loss-of-function mutations in genes associated with ribosome maturation, including *SBDS* (>90% of cases), *DNAJC21*, and *EFL1*, or by heterozygous mutations in *SRP54*.[11-15] In addition to exocrine pancreatic dysfunction, patients with SDS develop hematopoietic abnormalities, including BM hypocellularity, neutropenia, and variable thrombocytopenia. Approximately 20% to 25% of patients will develop severe cytopenias associated with BM aplasia, and 36% of patients will develop MDS/leukemia by age 30,[16,17] both requiring HSCT for cure. Unfortunately, HSCT for SDS is associated with significant rates of complications, including graft dysfunction, overt graft failure in up to 10% of patients,[18] conditioning-associated organ failure, and, for patients with MDS/leukemia, high relapse risk estimated at 20% to 30%.[19-21]

Skeletal dysplasia and osteopenia are also frequent manifestations of SDS,[22] suggesting that bone and OC dysfunction may be linked to hematopoietic dysfunction. Testing this hypothesis, previous studies in mouse models have shown that *SBDS* deficiency in osteolineage niche cells, but not hematopoietic cells, results in BM dysfunction, including myelodysplasia.[5,6,23] No murine models or clinical data to date address whether *SBDS* deficiency causes BM niche dysfunction that contributes to poor donor engraftment outcomes after HSCT.

Herein we detail development of a mouse model defined by inducible *Sbds* deletion in BM hematopoietic cells and OCs. Primary and secondary BM transplantation (BMT) studies revealed that SBDS deficiency within BM niches results in poor hematopoietic recovery and specifically poor donor HSC engraftment after myeloablative BMT. We identified molecular and cellular abnormalities driven by SBDS deficiency within post-myeloablation niches associated with this poor engraftment phenotype. These post-BMT conditioning niche abnormalities include altered frequencies of mesenchymal lineage cells, macrophages, and ECs and disruption of molecular signals in the niche, including growth factor signaling, cell adhesion and homing pathways, and cell cycle/cell death pathways. Our study reveals that BMT using traditional myeloablative conditioning is associated with severe BM niche dysfunction in the setting of SBDS deficiency and identifies niche pathways altered by SBDS deficiency that are critical for efficient engraftment after BMT.

Materials and methods

Animals and in vivo treatment

Mouse colonies were maintained under pathogen-free conditions. All experiments were conducted following protocols approved by Children's Hospital of Philadelphia Institutional Animal Care and Use Committee. $Sbds^{l/l}$ mice (mice with 2 copies of the $Sbds^{lox}$ allele) were generously provided by Dr. Johanna Rommens (University of Toronto). Other strains were either obtained from public repositories or purchased from Jackson Laboratory and backcrossed onto C57BL/6 background. $Mx1^{cre}Sbds^{l/l}$ mice were generated by crossing $Mx1^{cre}$ mice and $Sbds^{l/l}$ mice, confirming genotypes by polymerase chain reaction (PCR).[24] To induce *Sbds* deletion, polyinosinic-polycytidylic acid (pIpC, Sigma) was injected intraperitoneally (300 μg/mouse) 3 times per week for a minimum of 2 weeks. For green fluorescent protein $(GFP)^+$ donor BM for BMT, transgenic C57BL/6 mice expressing GFP under the H2K promoter (H2K-GFP) were used. Myeloablative total body irradiation (TBI) was performed using the X-RAD 320 (Precision X-ray) to deliver 1100 CGy in 2 fractions at least 3 hours apart.

Single-cell preparations from bone/BM

To prepare single BM cell suspensions, BM was flushed from leg bones, filtered (40-μm mesh) and subjected to red blood cell (RBC) lysis. To prepare single niche cell suspensions after BM flushing, leftover bones were cut into 1- to 2-mm pieces and digested at 37°C for 1 hour with collagenase P (Roche) or collagenase II (Gibco). Collected supernatants were filtered through 100-μm mesh. Cell counts were determined using a hematocytometer and Trypan Blue (Corning).

Quantitative PCR

To measure expression of *Sbds* transcripts, RNA was isolated from single cell suspensions using RNeasy Mini Kit (Qiagen). First-strand cDNA was synthesized by SuperScript III reverse transcription (Thermo Fisher Scientific). Quantitative PCR (qPCR) was performed on 7500 Fast Real-Time PCR System (Applied Biosystems) with SYBR Green PCR Master Mix (Applied Biosystems). Target-specific primers are described in supplemental Table 1.

Flow cytometry

Flow cytometry analysis was performed on FACSCalibur or FACSJazz (Becton Dickinson). Fluorophore-conjugated antibodies used are listed in supplemental Table 2.

BMT assays

In primary BMT assays, $Mx1^{cre}Sbds^{l/l}$ or $Sbds^{l/l}$ recipients received 1100 cGy TBI followed by 10^6 GFP^+ BM cells from H2K-GFP donors via retro-orbital injection. For competitive secondary BMT assays, 1 week after primary BMT, BM was collected from bilateral femorae/tibiae and pooled from ≥3 primary recipients per group. Pooled primary recipient BM (dose: one-fourth total BM volume collected from 1 primary recipient as detailed previously[4,10]) was injected into irradiated (1100 cGy) wild-type (WT) secondary recipients co-transplanted with GFP^{neg} 2×10^5 WT competitor BM cells. Secondary recipients were assessed 3 to 24 weeks after BMT for GFP^+ cell reconstitution in peripheral blood lineages, including RBCs, platelets, $Gr1^+$ myeloid cells, $B220^+$ B cells, and $CD3^+$ T cells.

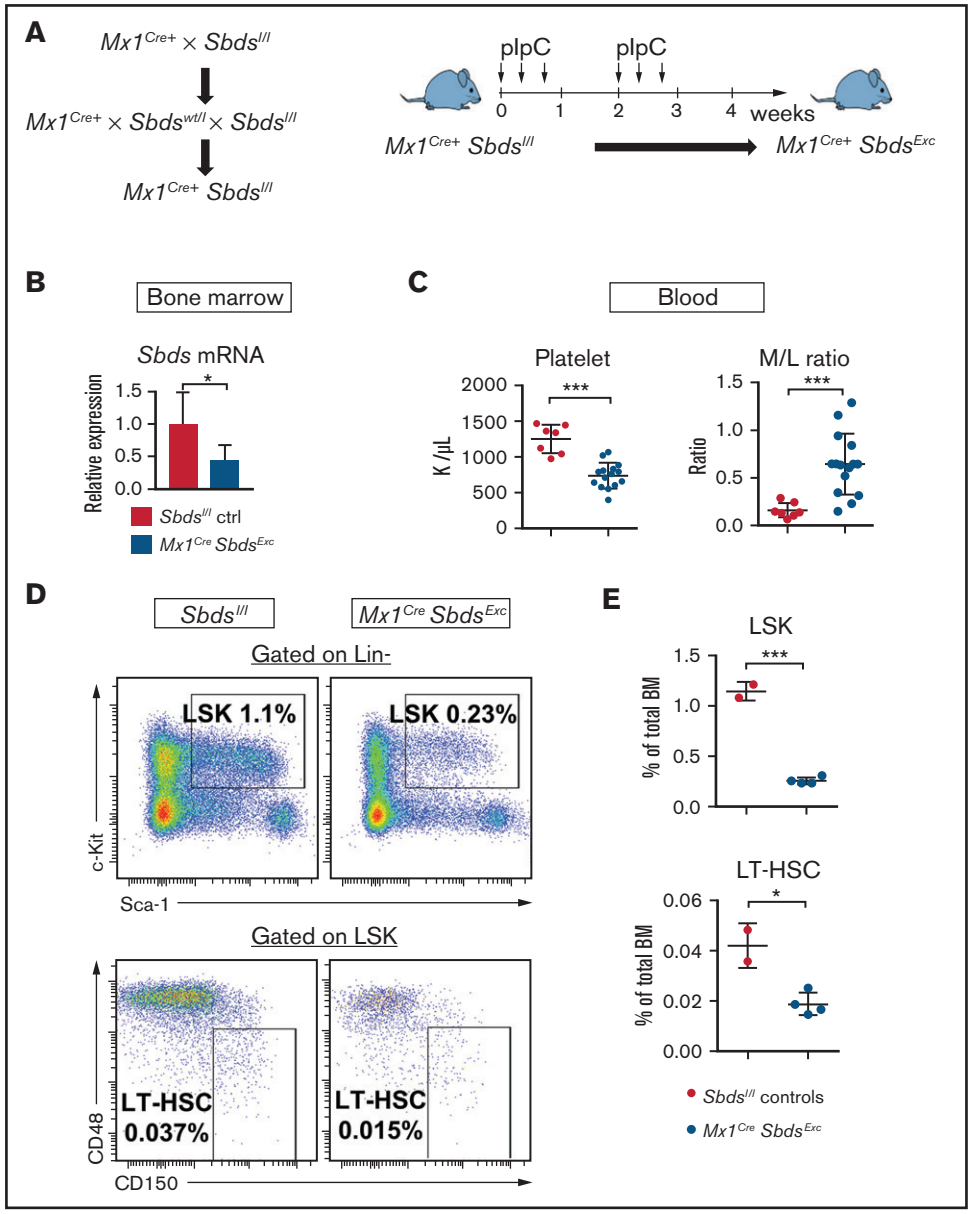

Figure 1. Mice with inducible SBDS deficiency in hematopoietic and osteolineage niche cells develop disrupted hematopoiesis consistent with BM failure. (A) *Mx1*^{Cre}*Sbds*^{Exc} mice were generated by crossing *Mx1*$^{Cre+}$ mice with *Sbds*$^{l/l}$ mice to generate *Mx1*$^{Cre+}$*Sbds*$^{l/l}$ mice. Cre expression and *Sbds* deletion were induced in hematopoietic and Mx1-inducible niche cells by pIpC treatment to create *Mx1*$^{Cre+}$*Sbds*^{Exc} mice. (B) After 4 weeks of pIpC treatment, qPCR demonstrated reduced Sbds mRNA expression in flushed BM cells compared with pIpC-treated *Sbds*$^{l/l}$ controls. (C) Compared with pIpC-treated control *Sbds*$^{l/l}$ mice (n = 7), *Mx1*^{Cre}*Sbds*^{Exc} mice (n = 12) developed reduced platelet counts and an increased peripheral blood myeloid/lymphoid (M/L) cell ratio, consistent with stress hematopoiesis. (D) Representative dot plots showing decreased percentages of lin$^-$Sca1$^+$cKit$^+$ (LSK) cells and CD48$^-$CD150$^+$ long-term HSC (LT-HSC) in total BM of *Mx1*^{Cre}*Sbds*^{Exc} vs control mice after 4 weeks of pIpC treatment. (E) *Mx1*^{Cre}*Sbds*^{Exc} BM (n = 2) shows severe reduction in percentages of LSK and LT-HSC compared with control BM (n = 4). *$P < .05$; ***$P < .001$; Student *t* test.

Histology and immunohistochemistry analysis

Femora and tibiae were fixed in 10% formalin and decalcified by Regular-Cal Immuno^M (BBC Biomedicals). Samples were dehydrated before embedding in paraffin and cut into 5- to 6-μm sections. For general histology analysis, sections were stained with Harris hematoxylin and eosin (Sigma-Aldrich). Immunostaining of PPAR-γ, Caspase-3, and CXCL12 was performed using primary antibodies listed in supplemental Table 2, along with goat anti-rabbit antibody, avidin/biotin, Vector Elite ABC kit, and DAB Substrate (Vector Laboratory) according to manufacturer's instructions. Slides were examined with Zeiss AxioStar Plus and Olympus DP72 microscopic imaging.

Multiplex enzyme-linked immunosorbent assay

After flushing bilateral tibiae and femora in fixed volumes of phosphate-buffered saline (same volume for each sample to

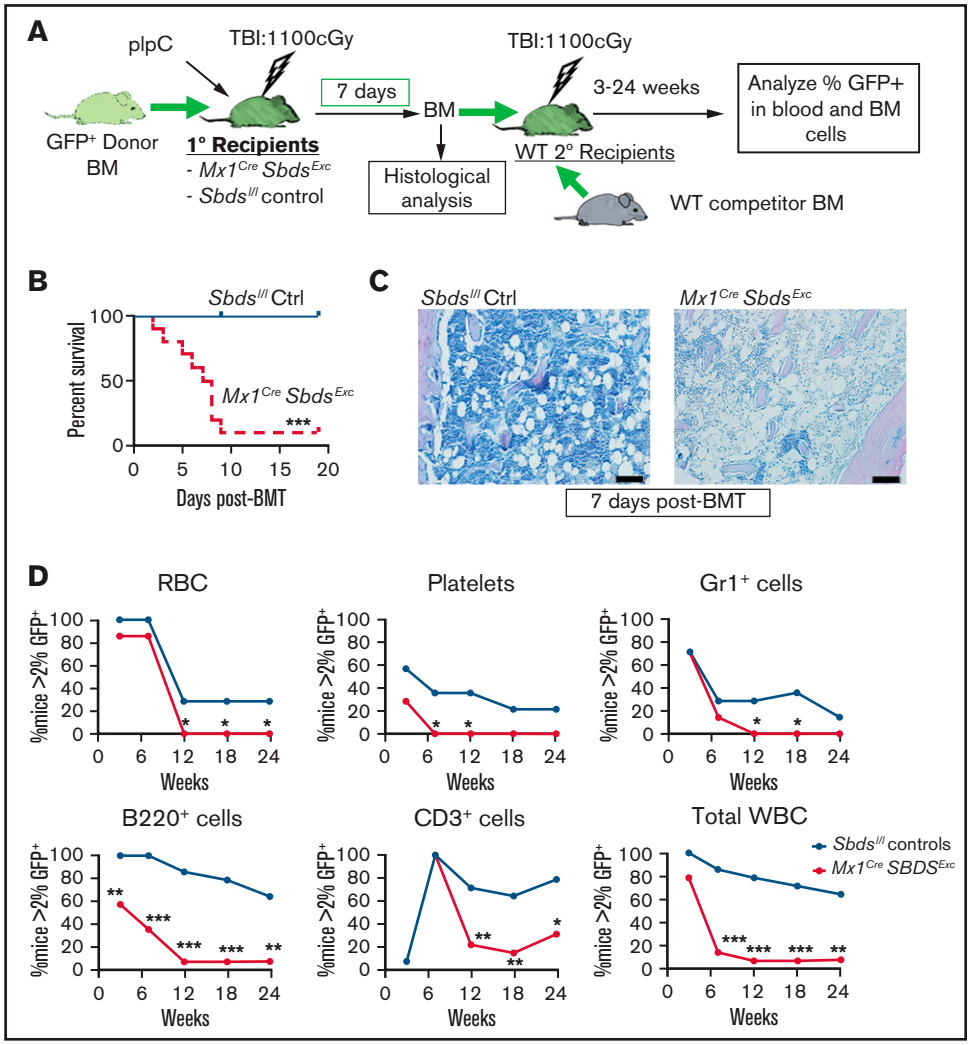

Figure 2. The BM niche of *Mx1*^{Cre}*Sbds*^{Exc} mice exhibits impaired capacity to engraft donor HSC after BMT. (A) Schematic of studies. *Mx1*^{Cre}*Sbds*^{Exc} mice and *Sbds*$^{///}$ controls received BMT of 10^6 whole BM from GFP$^+$ donor mice at 24 hours after receiving 1100 cGy of TBI. Donor engraftment in primary BMT recipients was assessed 1 week after primary BMT using histologic analysis and competitive secondary transplantation assays, in which defined volumes (25% of BM volume collected from bilateral hindleg bones) of whole BM from *Mx1*^{Cre}*Sbds*^{Exc} or *Sbds*$^{///}$ control primary recipients were transplanted with 2×10^5 WT competitor (GFP^{neg}) whole BM cells into irradiated WT secondary recipients. (B) Cumulative survival curves showed increased mortality among *Mx1*^{Cre}*Sbds*^{Exc} recipients (n = 10) after BMT compared with controls (n = 8). ***$P < .001$; log-rank test. (C) Impaired donor engraftment was seen in *Mx1*^{Cre}*Sbds*^{Exc} primary recipients by hematoxylin and eosin staining at 1 week after BMT. Scale bar: 200 μm. (D) In competitive secondary BMT studies, donor engraftment efficiency in *Mx1*^{Cre}*Sbds*^{Exc} or control (*Sbds*$^{///}$) primary recipients (n = 4 mice per group) was assessed by competitive secondary BMT assay. HSC and hematopoietic progenitor engraftment in primary recipient *Mx1*^{Cre}*Sbds*^{Exc} mice was significantly impaired, as indicated by lower GFP$^+$ reconstitution of secondary recipients (n = 14 mice per group) receiving *Mx1*^{Cre}*Sbds*^{Exc} vs control primary recipient BM in all blood lineages, including RBCs, platelets, Gr1$^+$myeloid cells, B220$^+$ B cells, CD3$^+$ T cells, and total white blood cells (WBC). *$P < .05$; **$P < .01$; ***$P < .001$; χ-squared test.

enable same dilution comparisons), samples were centrifuged at 400 × g for 5 minutes and BM plasma supernatants were separated. Cell fractions were lysed in phosphate-buffered saline containing 1% Nonidet-P40 (US Biological) and protease inhibitor (Roche). Lysates underwent 3 freeze-thaw cycles followed by centrifugation at 12 000 × g for 5 minutes. BM niche cell lysates were prepared after CD45$^+$ leukocyte depletion using anti-CD45 Microbeads (Miltenyi Biotec). Expression levels of 80 niche proteins were detected by Mouse Cytokine Array Q4 Kit, Mouse Cytokine Array Q5 Kit, and custom-designed Quantibody Mouse Array Kits (RayBiotech).

RNA-seq and bioinformatics analysis

After nonadherent BM was removed by flushing, leg bones were digested by collagenase. The cell suspension from digested bones was pooled together with the BM fraction after CD45$^+$ leukocyte depletion at baseline or after irradiation for RNA-sequencing (seq) analysis. The RNA was extracted from isolated BM and niche cell fractions using RNeasy Mini Kit (Qiagen), and DNA was removed using RNase-Free DNase Set (Qiagen). RNA-seq was performed by BGI Genomics (Hong Kong) on a BGISEQ-500 sequencer. Kallisto was used to perform pseudo-alignment and generated read counts defined as transcripts per million.[25] Differential gene expression was analyzed by *Deseq2*.[26] Gene set enrichment analysis

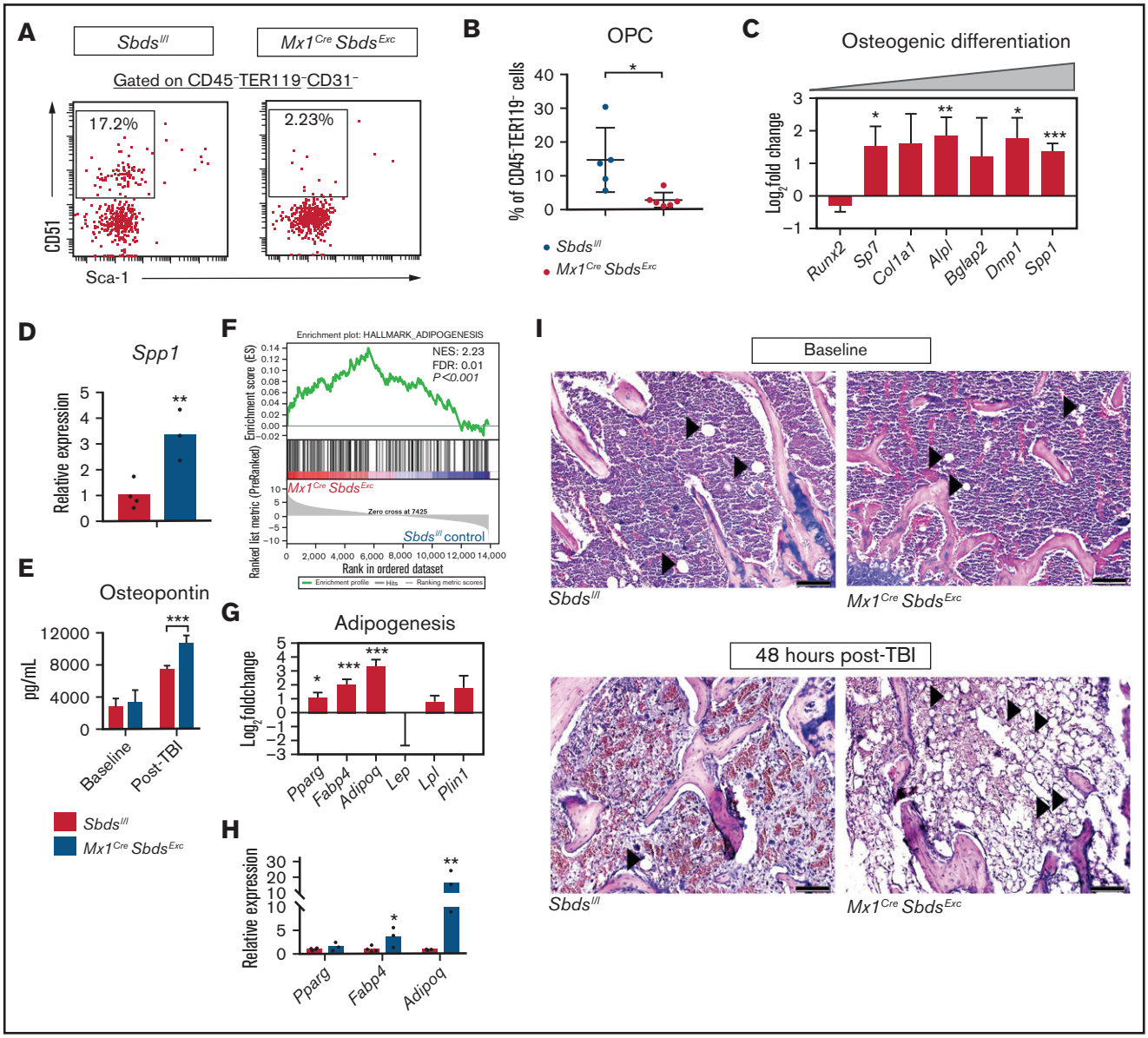

Figure 3. SBDS deficiency in BM niche cells results in decreased OPCs and increased adipocytes in BM after TBI. (A) Representative dot plots show gating strategies used to define CD31$^-$CD51$^+$Sca-1$^-$ OPCs in CD45$^-$TER119$^-$ BM stromal cells. (B) *Mx1*^{Cre}*Sbds*^{Exc} mice (n = 5) show reduced percentages of OPCs in CD45$^-$TER119$^-$ BM stromal cells compared with controls (n = 6) at 24 hours after 1100 cGy TBI. (C) RNA-seq analysis demonstrating changes of mRNA expression in genes critical for osteoblast differentiation in BM stromal cells of irradiated (24 hours after 1100 cGy TBI) *Mx1*^{Cre}*SBDS*^{Exc} vs control mice (n = 5 mice per group). A positive log-fold change in this plot indicates higher expression in *Mx1*^{Cre}*SBDS*^{Exc} stromal cells. (D) qPCR confirms higher expression of the terminal osteoblast marker *Spp1* (Osteopontin) in BM niche cells from irradiated (24 hours after 1100 cGy TBI) *Mx1*^{Cre}*Sbds*^{Exc} mice (n = 3) compared with controls (n = 4). (E) ELISA demonstrating increased osteopontin expression in BM plasma supernatants harvested from *Mx1*^{Cre}*SBDS*^{Exc} vs control mice 48 hours after 1100 cGy TBI (n = 5 for *Mx1*^{Cre}*SBDS*^{Exc} group and n = 6 for control group), but similar expression in the two groups at baseline (n = 5 for *Mx1*^{Cre}*SBDS*^{Exc} group; n = 7 for control group). (F) GSEA plot shows upregulation of adipogenesis-related gene expression in the BM stromal cells of irradiated (24 hours after 1100 cGy TBI) *Mx1*^{Cre}*SBDS*^{Exc} mice vs controls (n = 5 mice per group). The green line in the GSEA plot represents the running enrichment score (ES) for the gene set within the ranked list of genes. The value at the peak of the green line is the final ES. The black bars in the middle of the GSEA plot represent where the genes in the gene set appear in the ranked list. NES, normalized enrichment score; FDR, false-discovery rate. (G) Increased mRNA expression of several genes related to adipogenesis, including *Pparg*, *Fabp4*, and *Adipoq*, in the BM stromal cells of irradiated (24 hours after 1100 cGy TBI) *Mx1*^{Cre}*SBDS*^{Exc} mice compared with controls. (H) qPCR confirmed that BM niche cells from irradiated *Mx1*^{Cre}*Sbds*^{Exc} mice (n = 3) exhibit higher expression of *Fabp4* and *Adipoq*, which is critical for adipogenesis, compared with controls (n = 4) at 24 hours after 1100 cGy TBI. (I) Hematoxylin and eosin stains show increased adipocytes in BM from *Mx1*^{Cre}*SBDS*^{Exc} vs control mice at 48 hours after 1100 cGy TBI but not at baseline. Black arrowheads indicate adipocytes. Scale bar: 200 μm. *$P < .05$; **$P < .01$; ***$P < .001$; Student *t*-test or *DESeq2* statistical test.

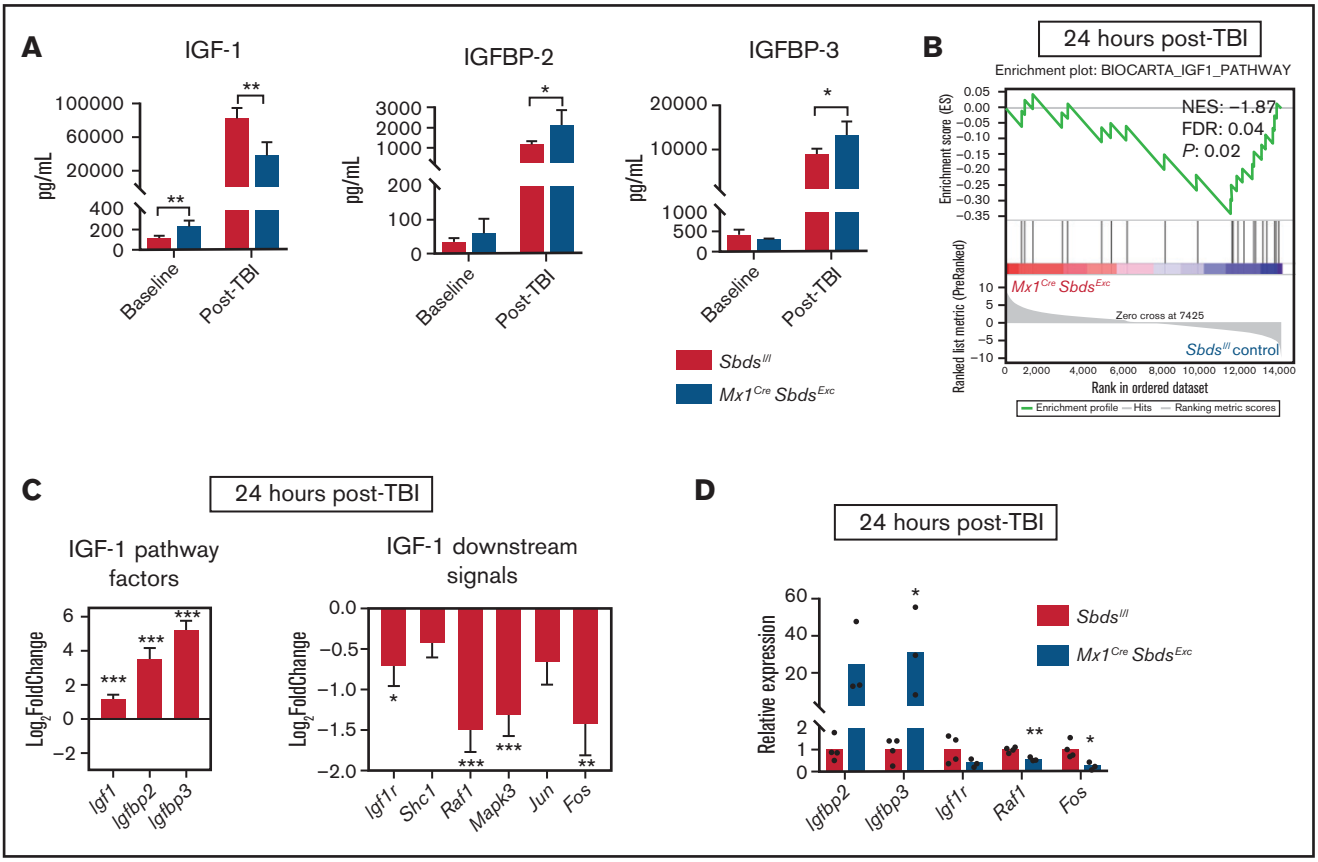

Figure 4. SBDS deficiency within BM niche cells diminishes gene expression downstream of IGF-1 signaling. (A) Protein expression of IGF-1, IGFBP-2, and IGFBP-3 in BM supernatants harvested from *Mx1*^{Cre}*SBDS*^{Exc} and control mice at baseline and 48 hours after 1100 cGy TBI (n ≥ 5 per group). *$P < .05$; **$P < .01$; Student *t*-test. (B) GSEA plot showing statistically significant alterations in IGF-1 signaling pathway gene expression in BM stromal cells from *Mx1*^{Cre}*SBDS*^{Exc} mice vs controls 24 hours after TBI (n = 5 per group). (C) Upregulation of upstream and downregulation of downstream signaling genes within the IGF-1 pathway in the BM stromal cells of irradiated *Mx1*^{Cre}*SBDS*^{Exc} mice compared with controls. *$P < .05$; **$P < .01$; ***$P < .001$; *DESeq2* statistical test. (D) qPCR validation confirms that BM niche cells from *Mx1*^{Cre}*Sbds*^{Exc} mice (n = 3) at 24 hours after 1100 cGy TBI show increased expression of IGF-1 factor genes *Igfbp2* and *Igfbp3*, along with decreased expression of downstream IGF-1 signaling pathway genes, including Raf1 and Fos, compared with irradiated controls (n = 4). *$P < .05$; **$P < .01$; Student *t*-test.

(GSEA) (Broad Institute) was performed using MSigDB C2 CP[27,28] and canonical pathway gene set collection (1027 gene sets). One thousand permutations were used to perform GSEA. GSEA plots were generated to provide a graphical view of enrichment scores.

Statistical analysis

Most statistical analyses were performed using GraphPad Prism 7.00. Student 2-tailed *t*-test or χ-squared tests were used to determine statistical significance of 2-group comparisons. For RNA-seq, statistical analysis was performed using the *DEseq2* package. Statistical methods for GSEA were performed with GSEA software from Broad Institute, including enrichment score calculation, significance level estimation, and adjustments for multiple hypothesis testing.[27] False-discovery rate <0.25 and *P* value <.05 were used as significance cutoff values.

Results

SBDS deficiency within BM niche cells impairs donor engraftment after BMT

A prior mouse model targeted *Sbds* deletion in Osterix-expressing osteolineage progenitors.[5,6] However, those mice only had a 4-week lifespan because of severe growth/development impairment, preventing that model's use for studying niche function during HSCT. We thus attempted to target *Sbds* in mature OCs by crossing previously described Sbds$^{f/f}$ mice[24] with *Col1a1*$^{Cre+}$ mice. However, *Col1a1*^{Cre}*Sbds*^{Exc} progeny exhibited embryonic lethality (supplemental Figure 1). We next generated a conditional *Sbds* deletion mouse model by crossing Sbds$^{f/f}$ mice with *Mx1*$^{Cre+}$ mice and inducing Cre expression in BM hematopoietic cells and *Mx1*-inducible osteolineage niche cells[29] using pIpC (Figure 1A). We first confirmed reduced, but not absent, *Sbds* gene expression in unsorted whole BM and isolated BM stromal cells from *Mx1*^{Cre} *Sbds*^{Exc} mice 4 weeks after pIpC initiation (Figure 1B; supplemental Figure 2A), similar to hypomorphic expression seen in clinical SDS.[30] Compared with controls, pIpC-treated *Mx1*^{Cre}*Sbds*^{Exc} mice develop significantly decreased platelet counts and an inverted myeloid/lymphoid white blood cell ratio in peripheral blood (Figure 1C; supplemental Figure 2B), indicative of stress hematopoiesis. Upon examining BM, both lin$^-$Sca1$^+$cKit$^+$ (LSK) progenitors and long-term (LT) HSC (lin$^-$Sca1$^+$cKit$^+$CD48$^-$CD150$^+$) were markedly reduced within 4 weeks of SBDS deficiency induction by pIpC in *Mx1*^{Cre}*Sbds*^{Exc} mice (Figure 1D-E).

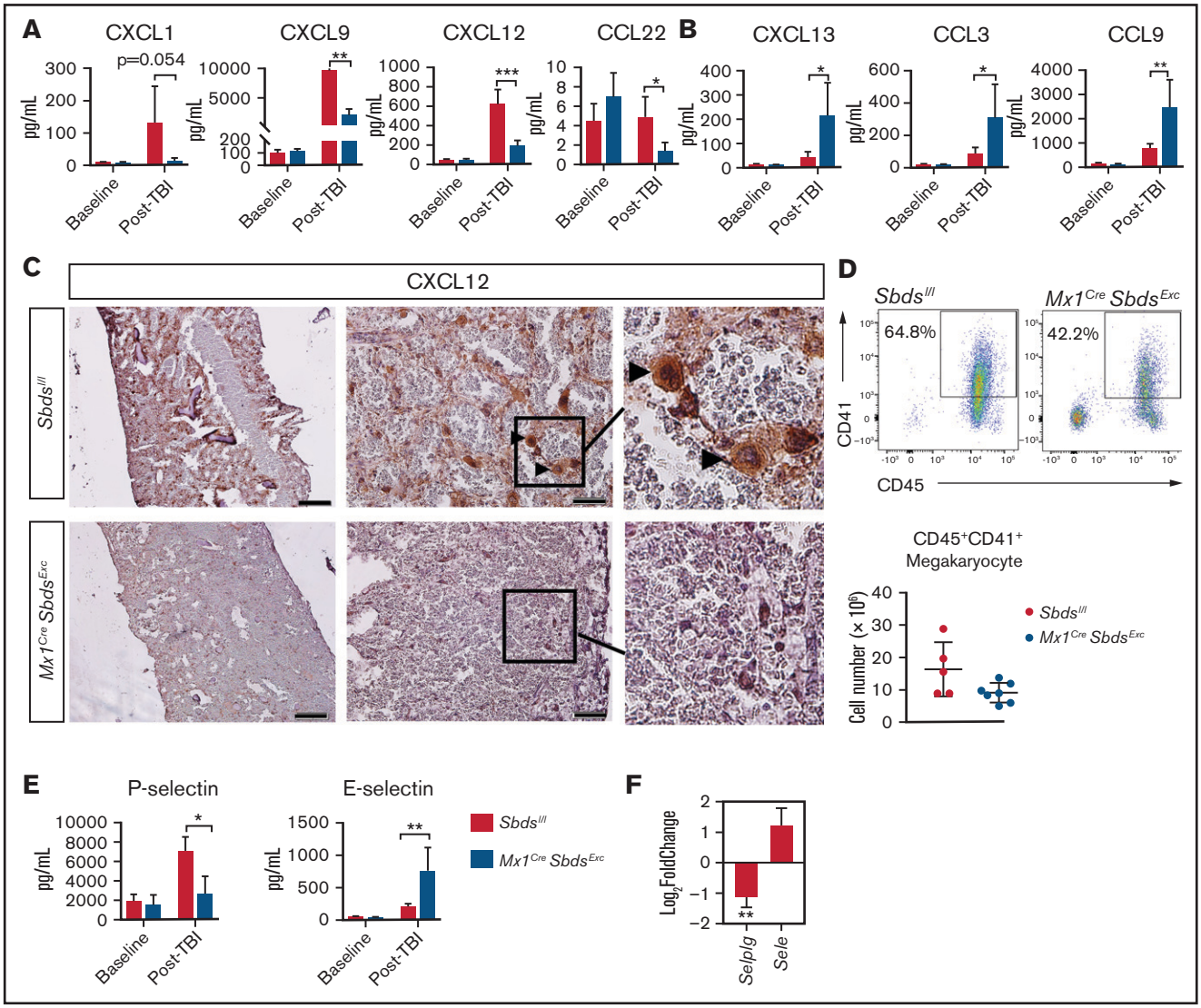

Figure 5. SBDS deficiency induces altered BM niche expression of chemokines and selectins after TBI that favor inflammatory cell recruitment. (A) CXCL1, CXCL9, CXCL12, and CCL22 expression by ELISA, demonstrating reductions in all 4 chemokines in BM plasma supernatants of *Mx1*^{Cre}*Sbds*^{Exc} (n = 5) vs control mice (n = 6) 48 hours after 1100-cGy TBI. (B) CXCL13, CCL3, and CCL9 expression by ELISA demonstrating increases in these proinflammatory chemokines in BM plasma harvested from *Mx1*^{Cre}*SBDS*^{Exc} (n = 5) vs controls (n = 6) at 48 hours after 1100-cGy TBI. (C) Immunohistochemistry staining demonstrates lower CXCL12 expression in BM from *Mx1*^{Cre}*Sbds*^{Exc} mice compared with controls at 48 hours after 1100-cGy TBI. Arrowheads indicate CXCL12-positivity surrounding megakaryocytes. Scale bar: 500 μm for the first column and 50 μm for the second column. (D) Representative dot plots (top) show gating strategies used to define CD45$^+$CD41$^+$ megakaryocytes in post-TBI BM. *Mx1*^{Cre}*SBDS*^{Exc} mice (n = 5) exhibit a trend toward decreased numbers of CD45$^+$CD41$^+$ megakaryocytes in the BM niche than controls (n = 7) at 24 hours after 1100-cGy TBI (bottom). $P = 0.06$; Student *t*-test. (E) P- and E-selectin levels by ELISA in BM cell lysates and BM supernatants, respectively, demonstrating lower P-selectin but higher E-selectin levels in *Mx1*^{Cre}*Sbds*^{Exc} (n = 5) vs control mice (n = 6) 48 hours after 1100-cGy TBI. (F) mRNA expression of *Selplg* (encodes P-selectin) and *Sele* (encodes E-selectin) in BM stromal cells of irradiated (24 hours after 1100-cGy TBI) *Mx1*^{Cre}*SBDS*^{Exc} mice compared with controls (n = 5 mice per group). *$P < .05$; **$P < .01$; ***$P < .001$; Student *t*-test used for ELISA data or *DESeq2* statistical test for RNA-seq data.

We next assessed whether SBDS deficiency within BM niche cell populations impacts capacity of pIpC-treated *Mx1*^{Cre}*Sbds*^{Exc} mice to engraft healthy donor BM and specifically LT-HSC during BMT. We transplanted GFP$^+$ WT donor BM into pIpC-treated *Mx1*^{Cre}*Sbds*^{Exc} mice and *Sbds*$^{I/I}$ controls at 24 hours after 1100 cGy myeloablative TBI (Figure 2A). Most (90%) *Mx1*^{Cre}*Sbds*^{Exc} BMT recipients died by day 9 after primary BMT, whereas all control recipients survived (Figure 2B). Inadequate engraftment appeared to be the cause of death in the *Mx1*^{Cre}*Sbds*^{Exc} recipients, demonstrated by the persistence of BM aplasia by histology (Figure 2C) and low BM cell counts (supplemental Figure 2C) at 1 week after BMT, compared with restored BM cellularity seen in control recipients. To test whether BM niche deficits caused by SBDS deficiency specifically impact engraftment of LT-HSC after BMT, we next performed competitive secondary BMT in which BM was harvested from *Mx1*^{Cre}*Sbds*^{Exc} and control primary BMT recipients at 7 days

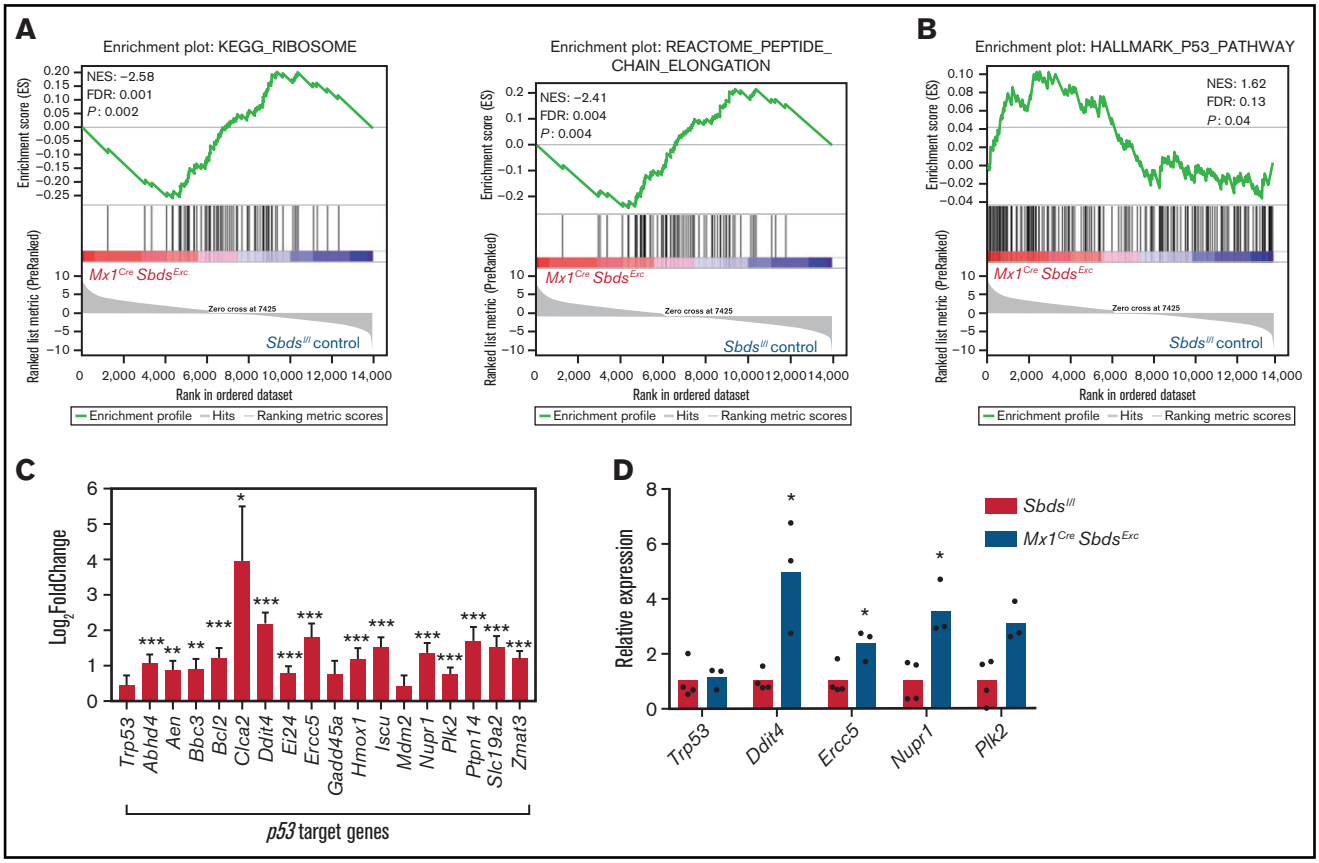

Figure 6. SBDS deficiency increases activation of p53 pathways in BM niche cells after myeloablative TBI. (A) GSEA plot showing overall downregulated expression of ribosomal proteins (left) and genes associated with peptide chain elongation (right) in BM stromal cells from irradiated (24 hours after 1100-cGy TBI) $Mx1^{Cre}SBDS^{Exc}$ mice vs irradiated controls. (B) GSEA plot shows overall increased activation of the p53 pathway in BM niches of irradiated $Mx1^{Cre}SBDS^{Exc}$ vs control mice (n = 5 mice per group). (C) Expression of individual p53 target genes is upregulated in BM niches of irradiated $Mx1^{Cre}SBDS^{Exc}$ vs control mice (n = 5 mice per group). FDR, false-discovery rate; NES, normalized enrichment score. *$P < .05$; **$P < .01$; ***$P < .001$; *DESeq2* statistical test. (D) qPCR confirms upregulation of these p53 target genes in BM niche cells taken from irradiated $Mx1^{Cre}SBDS^{Exc}$ (n = 3) vs control mice (n = 4) at 24 hours after 1100-cGy TBI. *$P < .05$; Student *t*-test.

after the primary BMT and transplanted with a fixed dose of competitor WT BM into WT secondary recipients. Secondary recipients of $Mx1^{Cre}Sbds^{Exc}$ vs littermate control primary recipient BM demonstrated decreased LT GFP^+ reconstitution of peripheral blood lineages from 6 to 24 weeks after secondary BMT as well as decreased trilineage GFP^+ BM hematopoiesis, indicating that engraftment of both hematopoietic progenitors and HSC was severely impaired in $Mx1^{Cre}Sbds^{Exc}$ vs littermate control primary recipients (Figure 2D; supplemental Figure 2D).

SBDS deficiency alters BM niche cellular composition and niche cell gene expression in response to myeloablative TBI

To define mechanisms by which SBDS deficiency in BM niches impairs HSCT donor engraftment, we compared niche cell populations and niche gene expression in $Mx1^{Cre}Sbds^{Exc}$ mice vs $Sbds^{f/f}$ controls after myeloablative TBI (experiment schema in supplemental Figure 3). We first investigated MSC-derived stromal compartments that contribute to BMF and MDS in other models,[5,6,8] finding that BM of irradiated $Mx1^{Cre}Sbds^{Exc}$ mice contains reduced osteoprogenitor cells (OPCs; $CD45^-TER119^-CD31^-CD51^+Sca\text{-}1^-$) compared with controls (Figure 3A-B), although the OPC percentage was not significantly altered at baseline (supplemental Figure 4A). Percentages of MSC ($CD45^-TER119^-CD31^-CD51^+Sca\text{-}1^+$) were similar between the two groups (data not shown). RNA-seq analysis revealed that BM stromal cells from irradiated $Mx1^{Cre}Sbds^{Exc}$ mice and controls expressed similar levels of *Runx2* (Figure 3C), which encodes the transcription factor that initially induces osteogenic differentiation of MSC. However, SBDS-deficient BM niche cells expressed higher levels of early osteoblast markers, including *Sp7* (Osterix) *and Alpl* (alkaline phosphatase), as well as terminal osteoblast markers, including *Dmp1* and *Spp1* (Osteopontin) (Figure 3C-D), suggesting that terminal osteoblast maturation and function may not be impaired by induced SBDS deficiency. Enzyme-linked immunosorbent assay (ELISA) confirmed increased BM osteopontin expression in irradiated $Mx1^{Cre}Sbds^{Exc}$ mice (Figure 3E). These results suggest that while signals driving osteolineage commitment of MSC remain intact and in some cases are upregulated in SBDS-deficient niches in response to myeloablative TBI, the ability to maintain populations of immature osteolineage-committed progenitor cells after TBI is severely impaired by SBDS deficiency, through either increased terminal differentiation or impaired survival.

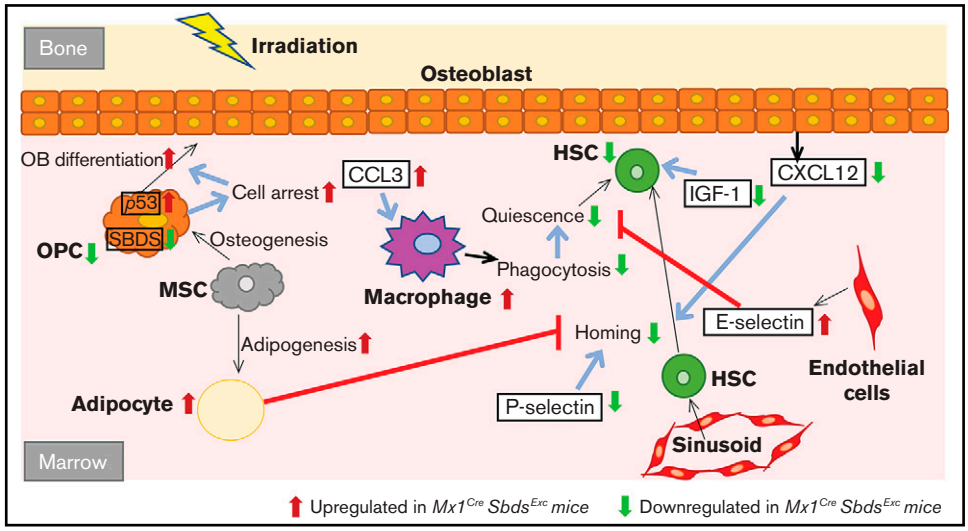

Figure 7. Schematic of how SBDS deficiency in the *Mx1*^{Cre}*SBDS*^{Exc} model impacts BM niche cell composition and gene expression in response to myeloablative irradiation, leading to impaired niche capacity to engraft donor HSC after HSCT. Our studies support a model by which *Sbds* knockdown in *Mx1*-inducible osteolineage niche cells impairs donor HSC engraftment after TBI. SBDS deficiency in osteoprogenitors causes ribosomal dysfunction, p53 pathway activation, and cell cycle arrest, which impairs the ability of these OCs to proliferate in response to IGF-1 and other growth factor signals after TBI and, consequently, to support donor hematopoiesis. Because of cell intrinsic or extrinsic mechanisms, SBDS deficiency in niche cells also increases adipocytes and decreases EC survival in the BM microenvironment after TBI, both of which may impair donor engraftment after HSCT. Decreased osteoprogenitor-derived CXCL12 and endothelial P-selectin expression may limit HSC homing and lodgment within BM niches after TBI. Elevation of CCL3 and endothelial E-selectin drives recruitment of inflammatory macrophages after TBI. The resulting proinflammatory environment may further disrupt engraftment and maintenance of donor HSPC.

GSEA demonstrated that *Sbds* deletion in post-TBI BM niche cells caused upregulation in gene expression associated with adipogenesis, including upregulation of *Pparg*, *Fabp4*, and *Adipoq* (Figure 3F-H; supplemental Table 3). Notably, GSEA did not detect alteration of adipogenesis pathways in *Mx1*^{Cre}*Sbds*^{Exc} mice at baseline (supplemental Figure 4B), suggesting that TBI induced a proadipogenic state in *Mx1*^{Cre}*Sbds*^{Exc} mice. Indeed, we identified increased adipocytes in BM sections of *Mx1*^{Cre}*Sbds*^{Exc} mice at 48 hours after TBI but not at baseline (Figure 3I). Most adipocytes in irradiated *Mx1*^{Cre}*Sbds*^{Exc} BM are PPAR-γ-positive (supplemental Figure 4C). Because previous studies have implicated BM adipocytes as the negative regulators of HSC engraftment,[31] increased adipogenic differentiation of BM niche MSC may contribute to poor niche-mediated donor engraftment resulting from SBDS deficiency.

In contrast, ECs comprised a significantly lower fraction of surviving niche cells in irradiated *Mx1*^{Cre}*Sbds*^{Exc} vs control BM (supplemental Figure 5A-B), notable because sinusoidal EC regeneration mediated by vascular endothelial growth factor receptor 2 (VEGFR2) signaling is essential for HSC engraftment after HSCT.[32] While VEGF-A protein levels in BM plasma supernatants were increased after TBI compared with baseline in both groups, *Mx1*^{Cre}*Sbds*^{Exc} BM exhibited a trend ($P = .15$) toward less TBI-driven increase than seen in control BM (supplemental Figure 5C). GSEA of RNA-seq data showed that while at baseline VEGF signaling pathway genes are markedly upregulated in the BM of *Mx1*^{Cre}*Sbds*^{Exc} mice vs controls, BM stromal cells of irradiated *Mx1*^{Cre}*Sbds*^{Exc} mice exhibit overall downregulation of the VEGF signaling pathway compared with controls (supplemental Figure 5D; supplemental Table 3). However, when examining expression of individual VEGF pathway genes within niche cells after irradiation, SBDS deficiency appears to have a complex effect, increasing expression of genes such as *Kdr*, which encodes VEGFR2, while decreasing expression of other downstream mediators (supplemental Figure 5E).

BM niche macrophages also critically regulate HSC maintenance.[33] CD11b^{+}F4/80^{+}Ly6G^{-} macrophages were significantly increased in irradiated *Mx1*^{Cre}*Sbds*^{Exc} BM niches compared with controls, in contrast to decreased surviving granulocytes seen in *Mx1*^{Cre}*Sbds*^{Exc} BM 24 hours after TBI (supplemental Figure 6A-B). RNA-seq confirmed higher expression of niche macrophage markers, including *Vcam-1*, *Slglec1* (CD169), and *Ackr1* (CD234),[33] in irradiated *Mx1*^{Cre}*Sbds*^{Exc} vs control niche cell populations (supplemental Figure 6C). Interestingly, despite increased expression of genes involved in phagocytic pathways at baseline and increased frequency of HSC niche macrophages after TBI in SBDS-deficient mice, GSEA of RNA-seq revealed significantly downregulated expression of Fcγ*R*-mediated phagocytosis pathway genes in irradiated *Mx1*^{Cre}*Sbds*^{Exc} BM niches (supplemental Figure 6D; supplemental Table 3) compared with controls, suggesting that SBDS deficiency alters functions of niche macrophages after TBI.

SBDS deficiency within BM niche cells diminishes gene expression downstream of IGF-1 signaling

Our previous studies demonstrated that BM niche insulin-like growth factor-1 receptor(IGF-1R) signaling is essential for osteolineage niche cell expansion after TBI and efficient donor HSC engraftment.[34] IGF-1/IGF-2 signaling pathways in the BM microenvironment also regulate homeostatic HSC function,[35,36] as prior studies have shown that IGFBP-2 and IGFBP-3 support HSC survival and inhibit OPC differentiation.[37-39] Compared with controls, BM plasma supernatants from *Mx1*^{Cre}*Sbds*^{Exc} mice

contained higher levels of IGF-1 at baseline but decreased levels of IGF-1 after TBI (Figure 4A). Protein levels of IGFBP-2 and IGFBP-3 were similar in *Mx1*^{Cre}*Sbds*^{Exc} mice vs controls at baseline, but *Mx1*^{Cre}*Sbds*^{Exc} BM exhibited increased levels of IGFBP-2 and IGFBP-3 after TBI (Figure 4A). Although baseline mRNA expression in IGF-1 pathway genes was similar with or without SBDS deficiency (supplemental Figure 7), RNA-seq analysis, GSEA, and qPCR of BM niche cells from irradiated *Mx1*^{Cre}*Sbds*^{Exc} vs control mice demonstrated upregulated mRNA expression of upstream IGF-1 pathway factors *Igf1*, *Igfbp2*, and *Igfbp3* but downregulated expression of downstream IGF-1 pathway signaling factors (Figure 4B-D). This downregulation of downstream IGF-1 signaling genes after TBI suggests that SBDS deficiency may impair this survival signal critical for OPC niche functions after HSCT.

BM niche SBDS deficiency during myeloablative TBI induces chemokine and adhesion molecule expression that favors inflammatory cell homing and impairs HSPC trafficking to BM

Chemokines and adhesion molecules play critical roles in donor HSC homing and retention within BM niches after HSCT. Hypothesizing that engraftment deficits in *Mx1*^{Cre}*Sbds*^{Exc} mice may be due to impaired chemokine and adhesion molecule pathways, we tested the effect of SBDS deficiency on 20 BM chemokines levels before and after TBI using multiplex ELISA (Figure 5A-B; supplemental Table 4). Although baseline chemokine levels were not altered by SBDS deficiency, 48 hours after irradiation, *Mx1*^{Cre}*Sbds*^{Exc} vs control BM demonstrated markedly reduced levels of 4 chemokines, including CXCL1, CXCL9, CXCL12, and CCL22, and elevated expression of 3 proinflammatory chemokines: CXCL13, CCL3, and CCL9 (Figure 5A-B). The upregulation of proinflammatory chemokines, particularly CCL3, in BM of irradiated *Mx1*^{Cre}*Sbds*^{Exc} mice may drive recruitment of proinflammatory macrophages and promote an inflammatory state that impairs normal hematopoiesis.[40-43] Notably, CXCL12 plays well-described critical roles driving engraftment of CXCR4-expressing donor HSC within BM niches after HSCT. CXCL12 is expressed by several cell populations within the marrow niche,[2] including OCs and ECs that were reduced in *Mx1*^{Cre}*Sbds*^{Exc} BM after TBI (Figure 3; supplemental Figure 5). We assessed localization of BM CXCL12 expression changes caused by SBDS deficiency after TBI using immunohistochemistry (Figure 5C). Control mice exhibited foci of high CXCL12 levels, colocalizing with large cells possessing the morphologic appearance of megakaryocytes, which are CXCL12-responsive niche cells that survive TBI for several days and promote engraftment after BMT.[4] In contrast, these clusters of high CXCL12 expression were absent in *Mx1*^{Cre}*Sbds*^{Exc} BM (Figure 5C), correlating with a trend toward reduction in surviving megakaryocytes in post-TBI *Mx1*^{Cre}*Sbds*^{Exc} BM (Figure 5D; $P = .06$). Reduced CXCL1 expression in post-TBI *Mx1*^{Cre}*Sbds*^{Exc} BM may also contribute to engraftment deficits. In a zebrafish model, CXCR1 ligands (of which mouse CXCL1 is a homolog[44]) play key supportive roles promoting donor HSPC engraftment.[45,46]

Endothelial expression of selectins also regulates HSC and inflammatory cell homing to BM niches.[2] After TBI, *Mx1*^{Cre}*Sbds*^{Exc} BM niche cells exhibited lower P-selectin and higher E-selectin protein and mRNA expression vs controls (Figure 5E-F). Because P-selectin expression on BM ECs is critical for constitutive HSPC homing[47] but endothelial E-selectin promotes homing of inflammatory cells and increases HSC proliferation at the expense of self-renewal,[48] dysregulated selectin expression in BM niche cells caused by SBDS deficiency may synergize with alterations in chemokine expression (Figure 5A-B) to promote inflammatory cell recruitment to BM at the expense of hematopoietic engraftment.

BM niche cells from *Mx1*^{Cre}*Sbds*^{Exc} mice demonstrate dysregulated ribosomal protein gene expression and P53 pathway activation after TBI

Multiple studies have demonstrated that aberrant p53 activation caused by ribosomal protein mutations is a critical driver of lineage-specific cell dysfunction in SDS and other ribosomopathies.[6,49] GSEA detected an overall downregulation in expression of genes critical for ribosomal biogenesis and protein translation in *Mx1*^{Cre}*Sbds*^{Exc} vs BM niche cells after myeloablative TBI (Figure 6A) but not in unirradiated BM stromal cells (supplemental Figure 8A). However, expression differences caused by SBDS deficiency in individual ribosomal genes after irradiation were in most cases not statistically significant (supplemental Figure 8B-C). Increased activation of p53 signaling pathways and upregulated expression of p53 target genes were seen in BM niche cells from *Mx1*^{Cre}*Sbds*^{Exc} vs control mice after TBI (Figure 6B-D; supplemental Table 3). In contrast, GSEA did not reach statistical significance comparing overall p53 pathway expression activation in unirradiated *Mx1*^{Cre}*Sbds*^{Exc} vs control niche cells at baseline (supplemental Figure 8D). SBDS deficiency caused downregulation of genes involved in G1/S transition and DNA synthesis in S-phase in the BM niche of *Mx1*^{Cre}*Sbds*^{Exc} mice both after radiation and at baseline (supplemental Figure 8E-F). These results suggest that baseline impairment in cell cycle transition within SBDS-deficient BM niche cells is exacerbated by ribosomal dysfunction-induced upregulation of p53 pathways after myeloablative conditioning. Higher percentages of apoptotic cells (Caspase-3^{+}) were also seen in the irradiated *Mx1*^{Cre}*Sbds*^{Exc} BM niche environment 48 hours after TBI (supplemental Figure 8G). Thus, cell cycle arrest and increased apoptosis within stromal cell populations may consequently impair niche capacity to efficiently engraft HSC after BMT.

Discussion

Although BMF in iBMFSs has long been attributed to HSPC-intrinsic impacts of causative germline gene mutations, increasing evidence suggests that impacts of these mutations on cells comprising BM microenvironmental niches also contribute to BMF.[4-9] Because SDS and other iBMFSs require HSCT to cure hematologic aspects of these diseases and because cytotoxic conditioning may exacerbate niche dysfunction caused by iBMFS-associated gene mutations, it is critical to understand pathophysiologic mechanisms by which BM niche capacity to engraft donor HSC is disrupted in iBMFSs. Because gene therapy approaches and novel nongenotoxic conditioning approaches are under development for iBMFSs,[50-52] better understanding of BM niche function intrinsic to certain gene mutations is critical for identifying optimal curative therapy approaches for iBMFSs.

We developed a murine model of SDS through conditional knockout of *Sbds* in *Mx1*-inducible hematopoietic and osteolineage niche cells to study SBDS-deficient BM niche function during HSCT. We demonstrated that SBDS-deficient BM niches possess reduced capacity to engraft healthy donor HSC after transplantation. SBDS

deficiency during myeloablative TBI led to marked alterations of BM niche cell composition, including increased adipocytes and macrophages and reduced OPCs and ECs. After myeloablative TBI, SBDS deficiency in BM niche cells disrupted IGF-1 signaling needed for OC remodeling of endosteal niches, decreased expression of chemokines and adhesion molecules known to drive HSC and progenitor cell homing to BM, and produced gene expression changes associated with ribosomal dysfunction, p53 activation, and increased cell cycle arrest in niche cells. Although future functional studies are needed to define relative contributions of gene expression changes in each of these pathways to niche-mediated engraftment deficits in this model, the diversity of pathways disrupted suggests that targeted correction of just one of these pathways may not be sufficient to restore donor HSC engraftment efficiency.

We used an inducible SDS mouse model to study BM niche deficits during HSCT because constitutive *Sbds* knockout models, including the $Col1a1^{Cre}Sbds^{Exc}$ model we initially attempted, have phenotypes too severe to allow for HSCT studies. This $Mx1^{Cre}Sbds^{Exc}$ has limitations in recapitulating human SDS, including the lack of developmental effects of SBDS deficiency, given that Cre recombinase activity was not induced until 6 weeks of age. $Mx1^{Cre}Sbds^{Exc}$ also did not develop neutropenia as is seen in human SDS, although absence of neutropenia has also been a feature of other murine SDS models.[5]

High mortality after receiving BMT in our SBDS-deficient mice may be fully explained by the graft failure phenotype we identified, but it is important to point out that we cannot exclude the possibility that alterations in other organ function after TBI could contribute to BMT-associated mortality in SBDS-deficient recipients.[53] Whereas reduced intensity conditioning, and not myeloablative TBI, is typically used as conditioning for HSCT in patients with SDS,[18] we chose myeloablative TBI as HSCT conditioning to define the maximal impact of conditioning on BM niche dysfunction in the setting of SBDS deficiency. Deficits seen in this study will serve as a benchmark for planned future studies to compare relative toxicities to BM niches induced by less intensive conditioning approaches, including non–TBI-based approaches.

Because of low survival rates of $Mx1^{Cre}Sbds^{Exc}$ recipients beyond 1 week after BMT, we could not determine whether poor niche function would result in permanent graft failure or delayed engraftment were the mice to survive the short-term consequences of prolonged aplasia, including severe anemia, bleeding, and infections. Although rates of graft failure are significant in clinical HSCT for SDS, most patients ultimately do engraft, suggesting that if similar niche dysfunction exists in human SDS, supportive care enables survival until engraftment ultimately occurs.

Previous studies demonstrated that Mx1-induced cells in BM stroma are restricted to osteolineage progenitor cells.[29] Therefore, targeting *Sbds* deletion using Mx1-Cre impacts niche function through cell autonomous function of osteolineage progenitors and nonautonomous effects on other niche cells. Our data indicate that $Mx1^{Cre}Sbds^{Exc}$ niches contain decreased OPCs after TBI but, interestingly, increased expression of genes required for terminal OPC differentiation. Although terminally differentiated osteoblasts may negatively regulate HSC pool size through production of osteopontin,[47,54] immature OPCs produce CXCL12 and other factors that promote HSC engraftment. The decrease in OCs after TBI caused by SBDS deficiency correlated with expansion of adipocytes known to inhibit efficient HSC engraftment,[31] reduction in BM EC that may also impair HSC engraftment,[32] and increased macrophages likely recruited through BM upregulation of proinflammatory chemokines (CCL3) and adhesion molecules (E-selectin) that may reduce survival and self-renewal of donor HSC.[48]

Finally, similar to the pathogenesis of BMF in SDS,[6] we found that SBDS deficiency in BM niche cells after TBI led to increased p53 activation and cell cycle arrest gene expression. Downregulation of ribosomal protein expression caused by SBDS deficiency in Mx1-inducible OPCs was the likely trigger of p53 pathway upregulation. Ribosomal dysfunction caused by SBDS deficiency may also impair poor engraftment through reduced protein expression of niche factors, such as CXCL12, due to broadly impaired protein translation.[55]

Taken together, our study demonstrates that the cell autonomous defects induced by SBDS deficiency within osteolineage niche cells disrupt multiple cellular and molecular elements in the BM microenvironment (Figure 7), ultimately leading to reduced BM niche capacity to engraft donor HSC during HSCT. Further studies are needed to define the relative contribution of these multiple affected pathways toward impaired donor engraftment and develop therapeutic strategies that target these pathways to improve engraftment outcomes.

Acknowledgments

The authors gratefully acknowledge Johanna Rommens for providing $Sbds^{lox/lox}$ mice and Peter Kurre for collaborative intellectual contributions to experiment design and manuscript review.

This work was supported by the National Heart, Lung, and Blood Institute, National Institutes of Health (grant K08HL122306), the American Society of Hematology Scholar Award, the Hyundai Hope on Wheels Scholar Hope Award, the W.W. Smith Charitable Foundation (T.S.O.), the Cure Childhood Cancer Foundation Cure Research Grant (T.S.O. and J.Z.), and National Heart, Lung, and Blood Institute, National Institutes of Health (grant K08HL132101) (D.V.B.).

Authorship

Contribution: J.Z. and T.S.O. conceived the studies, oversaw and personally performed the experiments, analyzed data, and wrote the manuscript; L.K.K. oversaw animal husbandry and assisted in conducting experiments; Y.B.S., X.Q., and J.-M.F. provided critical technical assistance in conducting experiments; H.M.X. and B.E. helped design and perform analysis for RNA-seq expression data; and D.V.B. critically reviewed studies in progress, contributed to manuscript editing, and provided valuable intellectual input to troubleshoot experiments and experimental design.

Conflict-of-interest disclosure: The authors declare no competing financial interests.

ORCID profiles: J.Z., 0000-0002-9365-9087; B.E., 0000-0002-2653-5009; D.V.B., 0000-0002-1745-0353; T.S.O., 0000-0003-1288-1960.

Correspondence: Timothy S. Olson, Blood and Marrow Transplant Program, Cell Therapy and Transplant Section, Children's Hospital of Philadelphia, Colket Translational Research Building, #3010, 3501 Civic Center Blvd, Philadelphia, PA 19104; e-mail: olsont@chop.edu.

References

1. Yu VWC, Scadden DTT. Hematopoietic stem cell and its bone marrow niche. *Curr Top Dev Biol.* 2016;118:21-44.
2. Olson TS. Translating HSC niche biology for clinical applications. *Curr Stem Cell Rep.* 2019;5(1):38-52.
3. Kaur S, Raggatt LJ, Millard SM, et al. Self-repopulating recipient bone marrow resident macrophages promote long-term hematopoietic stem cell engraftment. *Blood.* 2018;132(7):735-749.
4. Olson TS, Caselli A, Otsuru S, et al. Megakaryocytes promote murine osteoblastic HSC niche expansion and stem cell engraftment after radioablative conditioning. *Blood.* 2013;121(26):5238-5249.
5. Raaijmakers MHGP, Mukherjee S, Guo S, et al. Bone progenitor dysfunction induces myelodysplasia and secondary leukaemia. *Nature.* 2010; 464(7290):852-857.
6. Zambetti NA, Ping Z, Chen S, et al. Mesenchymal inflammation drives genotoxic stress in hematopoietic stem cells and predicts disease evolution in human pre-leukemia. *Cell Stem Cell.* 2016;19(5):613-627.
7. Li Y, Chen S, Yuan J, et al. Mesenchymal stem/progenitor cells promote the reconstitution of exogenous hematopoietic stem cells in Fancg-/- mice in vivo. *Blood.* 2009;113(10):2342-2351.
8. Zhou Y, He Y, Xing W, et al. An abnormal bone marrow microenvironment contributes to hematopoietic dysfunction in Fanconi anemia. *Haematologica.* 2017;102(6):1017-1027.
9. Bardelli D, Dander E, Bugarin C, et al. Mesenchymal stromal cells from Shwachman-Diamond syndrome patients fail to recreate a bone marrow niche in vivo and exhibit impaired angiogenesis. *Br J Haematol.* 2018;182(1):114-124.
10. Zha J, Kunselman LK, Fan J-MM, Olson TS. Bone marrow niches of germline FANCC/FANCG deficient mice enable efficient and durable engraftment of hematopoietic stem cells after transplantation. *Haematologica.* 2019;104(7):e284–e287.
11. Boocock GRB, Morrison JA, Popovic M, et al. Mutations in SBDS are associated with Shwachman-Diamond syndrome. *Nat Genet.* 2003;33(1): 97-101.
12. Tummala H, Walne AJ, Williams M, et al. DNAJC21 mutations link a cancer-prone bone marrow failure syndrome to corruption in 60s ribosome subunit maturation. *Am J Hum Genet.* 2016;99(1):115-124.
13. Stepensky P, Chacón-Flores M, Kim KH, et al. Mutations in *EFL1*, an *SBDS* partner, are associated with infantile pancytopenia, exocrine pancreatic insufficiency and skeletal anomalies in a Shwachman-Diamond like syndrome. *J Med Genet.* 2017;54(8):558-566.
14. Carapito R, Konantz M, Paillard C, et al. Mutations in signal recognition particle SRP54 cause syndromic neutropenia with Shwachman-Diamond-like features. *J Clin Invest.* 2017;127(11):4090-4103.
15. Bellanné-Chantelot C, Schmaltz-Panneau B, Marty C, et al. Mutations in the *SRP54* gene cause severe congenital neutropenia as well as Shwachman-Diamond-like syndrome. *Blood.* 2018;132(12):1318-1331.
16. Donadieu J, Fenneteau O, Beaupain B, et al; Associated investigators of the French Severe Chronic Neutropenia Registry. Classification of and risk factors for hematologic complications in a French national cohort of 102 patients with Shwachman-Diamond syndrome. *Haematologica.* 2012; 97(9):1312-1319.
17. Kennedy AL, Shimamura A. Genetic predisposition to MDS: clinical features and clonal evolution. *Blood.* 2019;133(10):1071-1085.
18. Myers K, Hebert K, Antin J, et al. Hematopoietic stem cell transplantation for Shwachman-Diamond syndrome. *Biol Blood Marrow Transplant.* 2020;26(8):1446-1451.
19. Kallen ME, Dulau-Florea A, Wang W, Calvo KR. Acquired and germline predisposition to bone marrow failure: diagnostic features and clinical implications. *Semin Hematol.* 2019;56(1):69-82.
20. Cesaro S, Pegoraro A, Sainati L, et al. A prospective study of hematologic complications and long-term survival of Italian patients affected by Shwachman-Diamond syndrome. *J Pediatr.* 2020;219:196-201.e1.
21. Nelson AS, Myers KC. Diagnosis, treatment, and molecular pathology of Shwachman-Diamond syndrome. *Hematol Oncol Clin North Am.* 2018; 32(4):687-700.
22. Myers KC, Davies SM, Shimamura A. Clinical and molecular pathophysiology of Shwachman-Diamond syndrome: an update. *Hematol Oncol Clin North Am.* 2013;27(1):117-128.
23. Zambetti NA, Bindels EMJJ, Van Strien PMHH, et al. Deficiency of the ribosome biogenesis gene Sbds in hematopoietic stem and progenitor cells causes neutropenia in mice by attenuating lineage progression in myelocytes. *Haematologica.* 2015;100(10):1285-1293.
24. Tourlakis ME, Zhong J, Gandhi R, et al. Deficiency of Sbds in the mouse pancreas leads to features of Shwachman-Diamond syndrome, with loss of zymogen granules. *Gastroenterology.* 2012;143(2):481-492.
25. Bray NL, Pimentel H, Melsted P, Pachter L. Near-optimal probabilistic RNA-seq quantification [published correction appears in Nat Biotechnol. 2016;34:888]. *Nat Biotechnol.* 2016;34(5):525-527.
26. Love MI, Huber W, Anders S. Moderated estimation of fold change and dispersion for RNA-seq data with DESeq2. *Genome Biol.* 2014;15(12):550.
27. Subramanian A, Tamayo P, Mootha VK, et al. Gene set enrichment analysis: a knowledge-based approach for interpreting genome-wide expression profiles. *Proc Natl Acad Sci USA.* 2005;102(43):15545-15550.
28. Mootha VK, Lindgren CM, Eriksson KF, et al. PGC-1α-responsive genes involved in oxidative phosphorylation are coordinately downregulated in human diabetes. *Nat Genet.* 2003;34(3):267-273.

29. Park D, Spencer JA, Koh BI, et al. Endogenous bone marrow MSCs are dynamic, fate-restricted participants in bone maintenance and regeneration. *Cell Stem Cell.* 2012;10(3):259-272.

30. Ganapathi KA, Austin KM, Lee CS, et al. The human Shwachman-Diamond syndrome protein, SBDS, associates with ribosomal RNA. *Blood.* 2007;110(5):1458-1465.

31. Naveiras O, Nardi V, Wenzel PL, Hauschka PV, Fahey F, Daley GQ. Bone-marrow adipocytes as negative regulators of the haematopoietic microenvironment. *Nature.* 2009;460(7252):259-263.

32. Hooper AT, Butler JM, Nolan DJ, et al. Engraftment and reconstitution of hematopoiesis is dependent on VEGFR2-mediated regeneration of sinusoidal endothelial cells. *Cell Stem Cell.* 2009;4(3):263-274.

33. Kaur S, Raggatt LJ, Batoon L, Hume DA, Levesque JP, Pettit AR. Role of bone marrow macrophages in controlling homeostasis and repair in bone and bone marrow niches. *Semin Cell Dev Biol.* 2017;61:12-21.

34. Caselli A, Olson TS, Otsuru S, et al. IGF-1-mediated osteoblastic niche expansion enhances long-term hematopoietic stem cell engraftment after murine bone marrow transplantation. *Stem Cells.* 2013;31(10):2193-2204.

35. Abu-Khader A, Law KW, Jahan S, et al. Paracrine factors released by osteoblasts provide strong platelet engraftment properties. *Stem Cells.* 2019; 37(3):345-356.

36. Young K, Eudy E, Bell R, et al. Decline in IGF1 in the bone marrow microenvironment initiates hematopoietic stem cell aging. *Cell Stem Cell.* 2021; 28(8):1473-1482.e7.

37. Huynh H, Zheng J, Umikawa M, et al. IGF binding protein 2 supports the survival and cycling of hematopoietic stem cells. *Blood.* 2011;118(12): 3236-3243.

38. Li J, Jin D, Fu S, et al. Insulin-like growth factor binding protein-3 modulates osteoblast differentiation via interaction with vitamin D receptor. *Biochem Biophys Res Commun.* 2013;436(4):632-637.

39. Eguchi K, Akiba Y, Akiba N, Nagasawa M, Cooper LF, Uoshima K. Insulin-like growth factor binding protein-3 suppresses osteoblast differentiation via bone morphogenetic protein-2. *Biochem Biophys Res Commun.* 2018;507(1-4):465-470.

40. Mirantes C, Passegué E, Pietras EM. Pro-inflammatory cytokines: emerging players regulating HSC function in normal and diseased hematopoiesis. *Exp Cell Res.* 2014;329(2):248-254.

41. Li AJ, Calvi LM. The microenvironment in myelodysplastic syndromes: niche-mediated disease initiation and progression. *Exp Hematol.* 2017;55:3-18.

42. Ntanasis-Stathopoulos I, Fotiou D, Terpos E. CCL3 signaling in the tumor microenvironment. *Adv Exp Med Biol.* 2020;1231:13-21.

43. Schepers K, Pietras EM, Reynaud D, et al. Myeloproliferative neoplasia remodels the endosteal bone marrow niche into a self-reinforcing leukemic niche. *Cell Stem Cell.* 2013;13(3):285-299.

44. Hol J, Wilhelmsen L, Haraldsen G. The murine IL-8 homologues KC, MIP-2, and LIX are found in endothelial cytoplasmic granules but not in Weibel-Palade bodies. *J Leukoc Biol.* 2010;87(3):501-508.

45. Calkins DL, Shaffer JL, Teets EM, et al. Cxcl8 expands hematopoietic stem and progenitor cells and alters their interaction with the endothelial niche. *Blood.* 2019;134(suppl 1):527.

46. Blaser BW, Moore JL, Hagedorn EJ, et al. CXCR1 remodels the vascular niche to promote hematopoietic stem and progenitor cell engraftment. *J Exp Med.* 2017;214(4):1011-1027.

47. Kim S, Lin L, Brown GAJ, Hosaka K, Scott EW. Extended time-lapse in vivo imaging of tibia bone marrow to visualize dynamic hematopoietic stem cell engraftment. *Leukemia.* 2017;31(7):1582-1592.

48. Winkler IG, Barbier V, Nowlan B, et al. Vascular niche E-selectin regulates hematopoietic stem cell dormancy, self renewal and chemoresistance. *Nat Med.* 2012;18(11):1651-1657.

49. Mills EW, Green R. Ribosomopathies: there's strength in numbers. *Science*. 2017;358(6363):eaan2755.

50. Liu JM, Kim S, Read EJ, et al. Engraftment of hematopoietic progenitor cells transduced with the Fanconi anemia group C gene (FANCC). *Hum Gene Ther.* 1999;10(14):2337-2346.

51. Kelly PF, Radtke S, von Kalle C, et al. Stem cell collection and gene transfer in Fanconi anemia. *Mol Ther.* 2007;15(1):211-219.

52. Adair JE, Chandrasekaran D, Sghia-Hughes G, et al. Novel lineage depletion preserves autologous blood stem cells for gene therapy of Fanconi anemia complementation group A. *Haematologica.* 2018;103(11):1806-1814.

53. Finch AJ, Hilcenko C, Basse N, et al. Uncoupling of GTP hydrolysis from eIF6 release on the ribosome causes Shwachman-Diamond syndrome. *Genes Dev.* 2011;25(9):917-929.

54. Stier S, Ko Y, Forkert R, et al. Osteopontin is a hematopoietic stem cell niche component that negatively regulates stem cell pool size. *J Exp Med.* 2005;201(11):1781-1791.

55. Calamita P, Miluzio A, Russo A, et al. SBDS-deficient cells have an altered homeostatic equilibrium due to translational inefficiency which explains their reduced fitness and provides a logical framework for intervention. *PLoS Genet.* 2017;13(1):e1006552.